Transformation of polyethylene into a vitrimer by nitroxide radical coupling of a bis-dioxaborolane

Florent Caffy and Renaud Nicolaÿ*

Chimie Moléculaire, Macromoléculaire, Matériaux. ESPCI Paris, CNRS, PSL University, 75005 Paris, France
Corresponding author email: renaud.nicolay@espci.psl.eu

Supporting Information

Contents

1. NMR characterization of TEMPO-BE and Bis-TEMPO-BE p.2
2. Grafting characterization by FTIR spectroscopy p 4
3. Photographs of HDPE, PE-V1 and PE-V2 p. 6
4. Quantification of the degree of crystallinity by DSC p. 7
5. Stress relaxation on PE-V1 and zero shear viscosities of HDPE, PE-V1 and PE-V2 p. 8
6. FTIR characterization of PE-V1 and PE-V2 after annealing at 250 °C p. 9
7. Strain sweep experiments on PE-V1 and PE-V2 p. 10
8. Mechanical properties of HDPE, PE-V1 and PE-V2 p. 11

1. NMR characterization of TEMPO-BE and Bis-TEMPO-BE

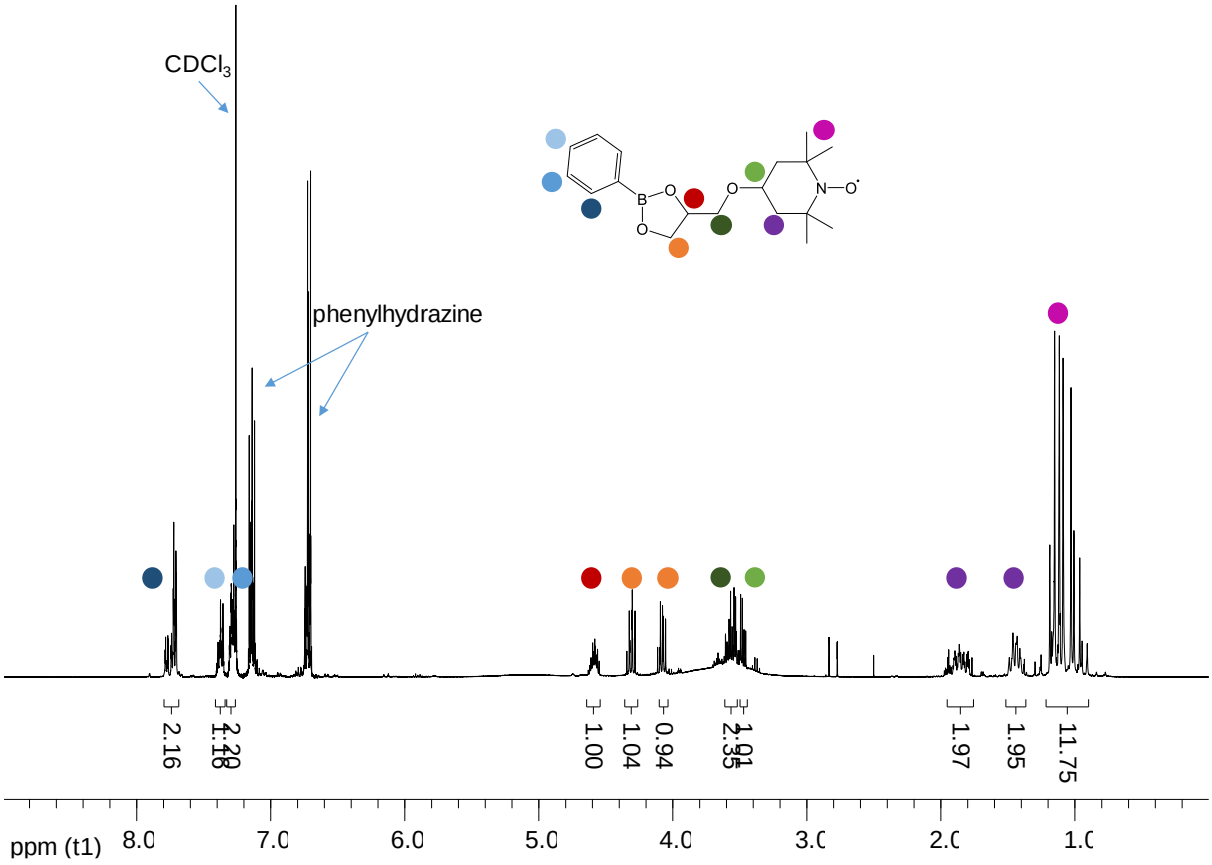

Fig. S1 ^{1}H NMR spectrum of TEMPO-BE in $CDCl_3$, in the presence of phenylhydrazine.

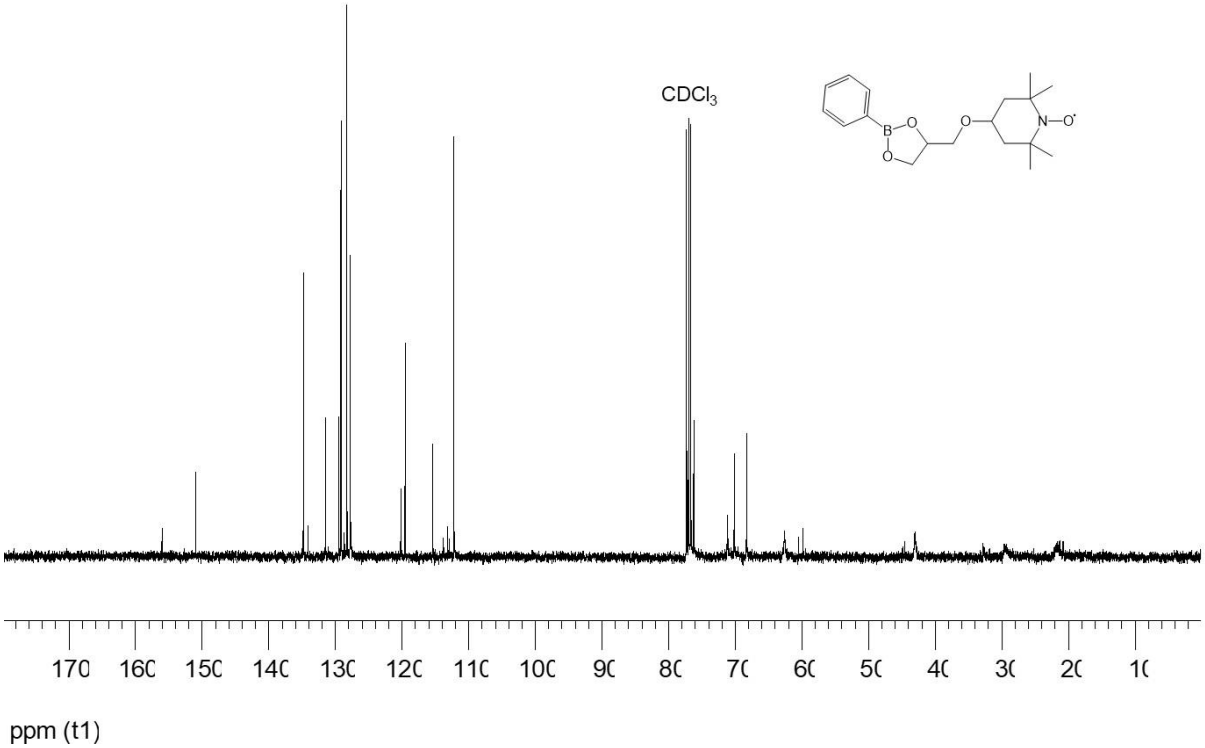

Fig. S2 ^{13}C NMR spectrum of TEMPO-BE in $CDCl_3$, in the presence of phenylhydrazine.

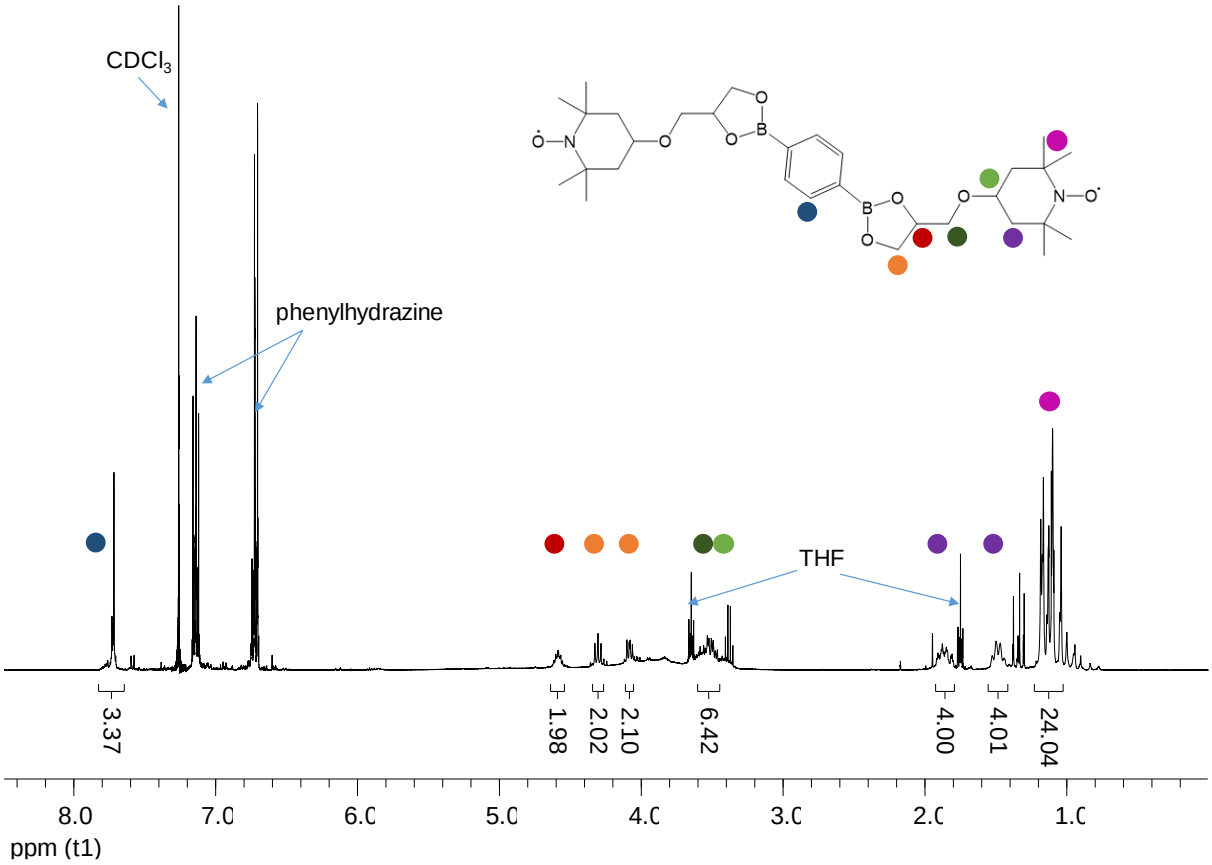

Fig. S3 ^{1}H NMR spectrum of Bis-TEMPO-BE in $CDCl_3$, in the presence of phenylhydrazine.

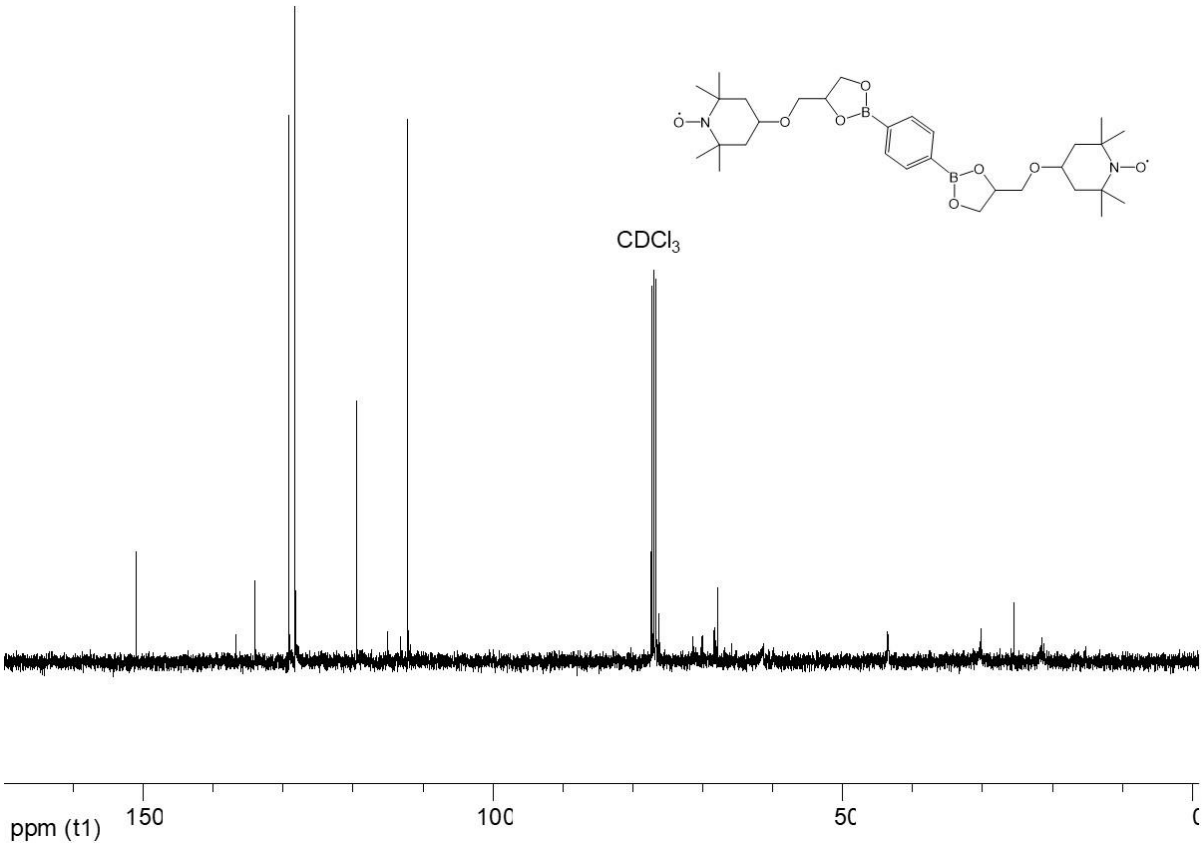

Fig. S4 ^{13}C NMR spectrum of Bis-TEMPO-BE in $CDCl_3$, in the presence of phenylhydrazine.

2. Grafting characterization by FTIR spectroscopy

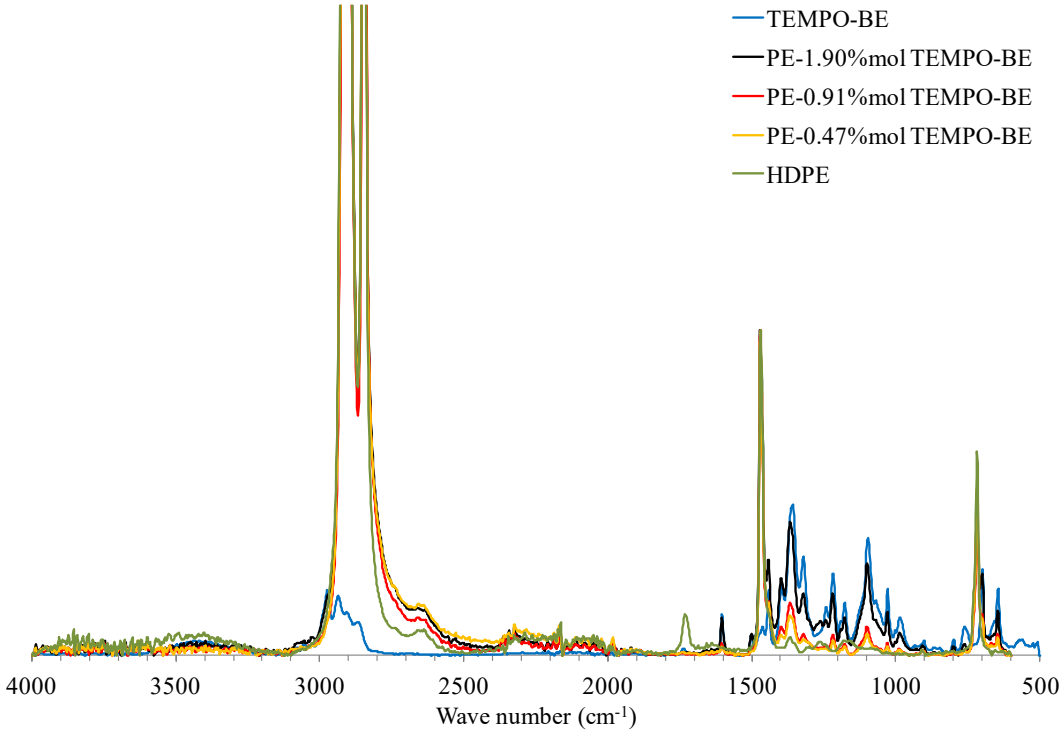

Fig. S5 FTIR spectra of HDPE, TEMPO-BE grafting agent and physical mixtures of HDPE with varying amounts of TEMPO-BE.

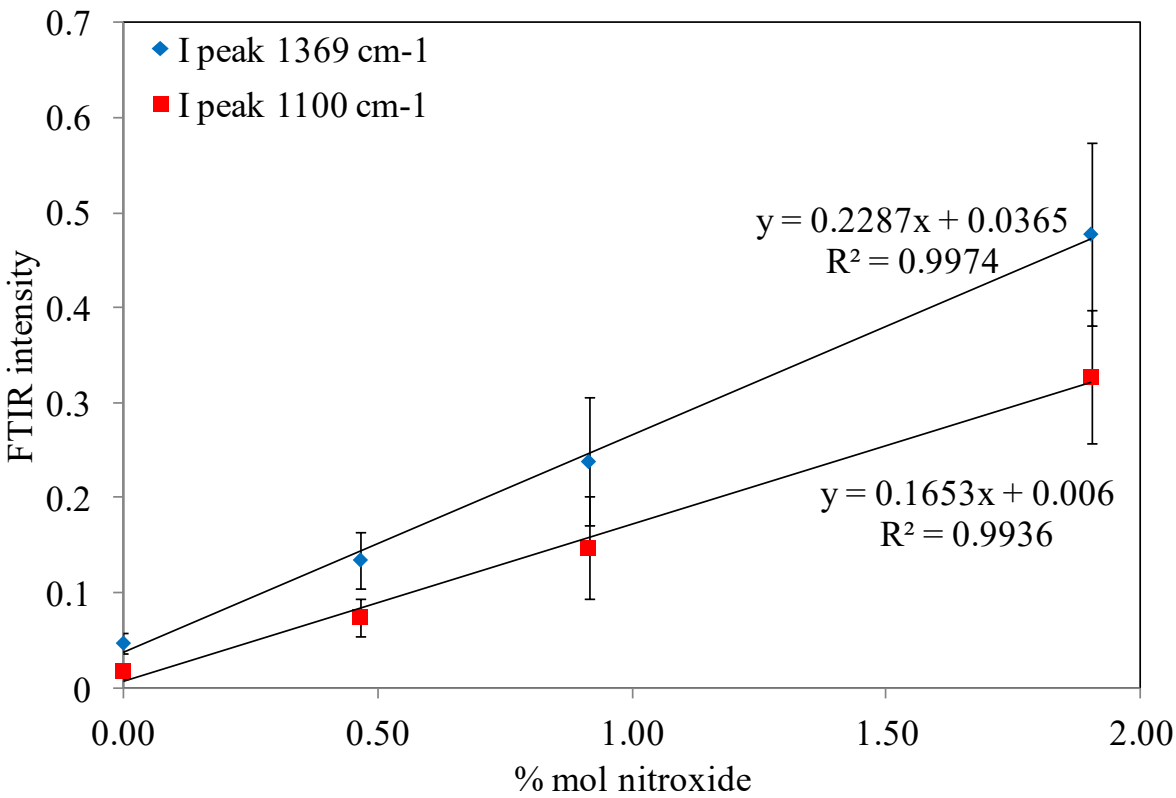

Fig. S6 FTIR intensity of B-O (1359 cm^{-1}) (blue) and B-C (1100 cm^{-1}) (red) vibration bands of TEMPO-BE as a function of the molar ratio of TEMPO-BE. Average on 3 samples.

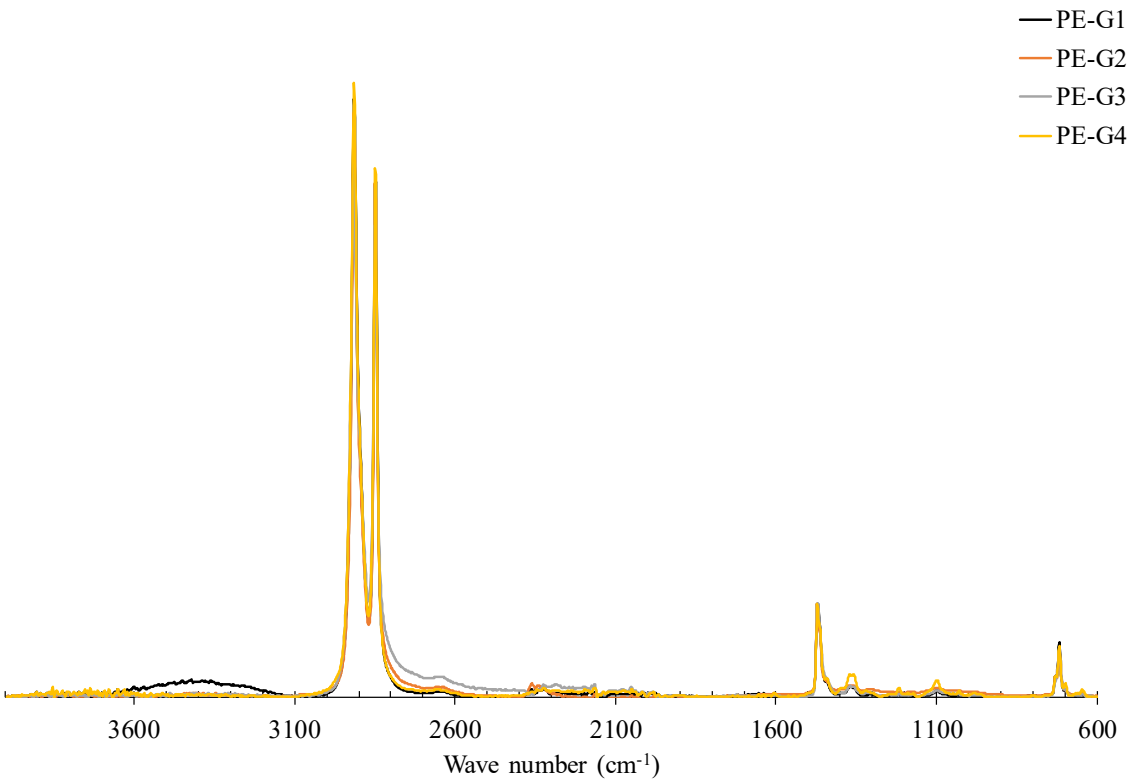

Fig. S7 FTIR spectra of HDPE grafted with TEMPO-BE: PE-G1, PE-G2, PE-G3 and PE-G4.

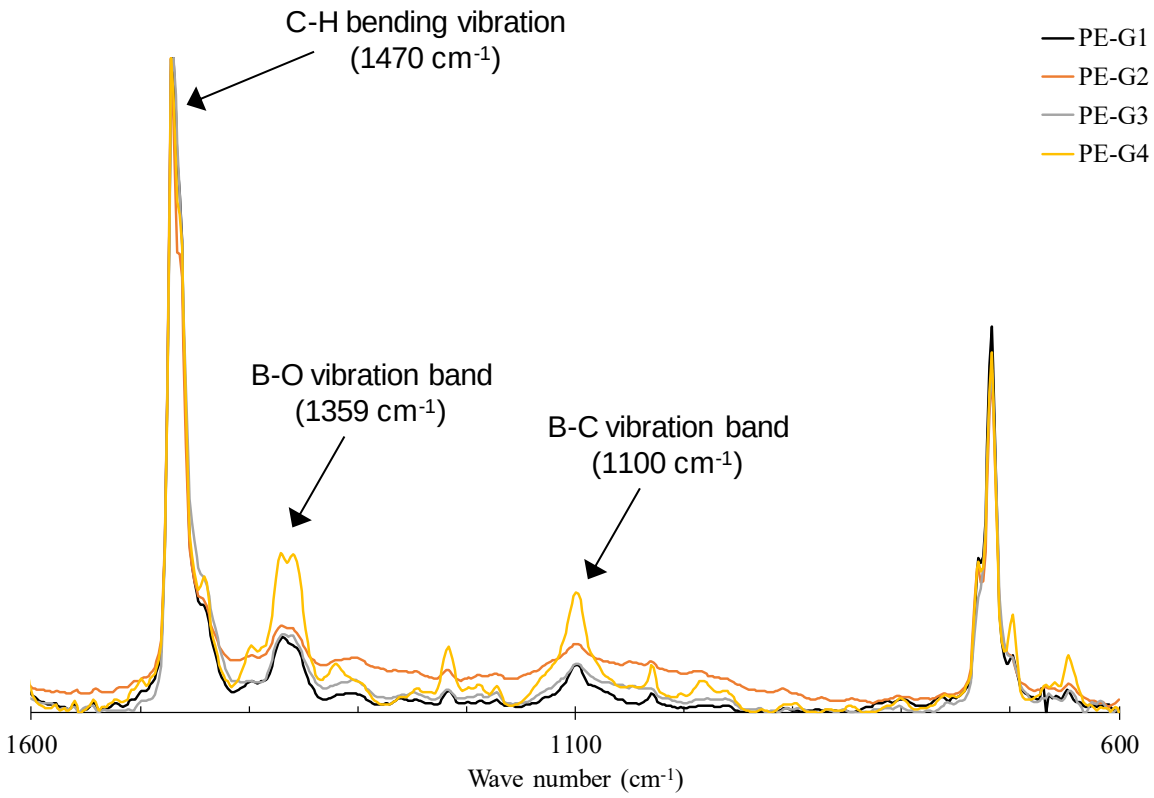

Fig. S8 FTIR spectra of HDPE grafted with TEMPO-BE: PE-G1, PE-G2, PE-G3 and PE-G4.

The degree of functionalization of grafted HDPE was calculated using the equations provided in Fig. S6 and normalizing the C-H bending vibration (1470 cm^{-1}) of PE to an intensity of 1.

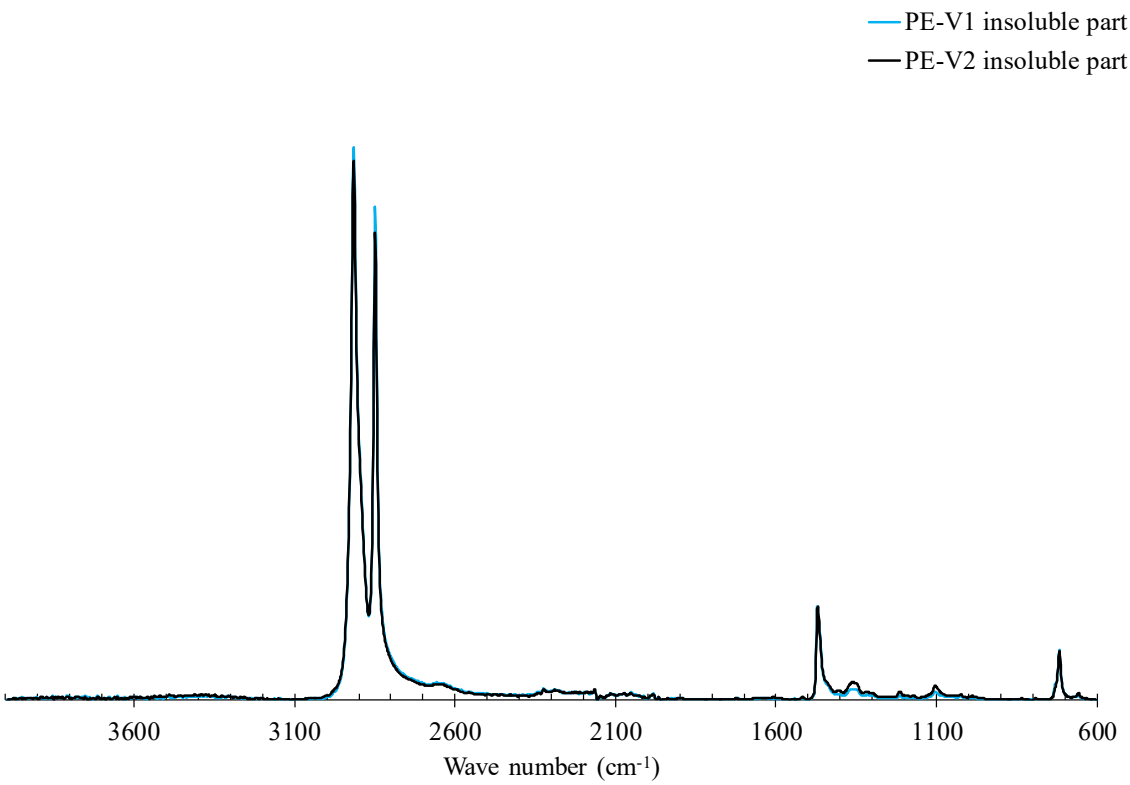

Fig. S9 FTIR spectra of the insoluble part of PE-V1 and PE-V2.

The degree of functionalization of HDPE vitrimers was calculated using the equations provided in Fig. S6 and normalizing the C-H bending vibration (1470 cm^{-1}) of PE to an intensity of 1.

3. Photographs of HDPE, PE-V1 and PE-V2

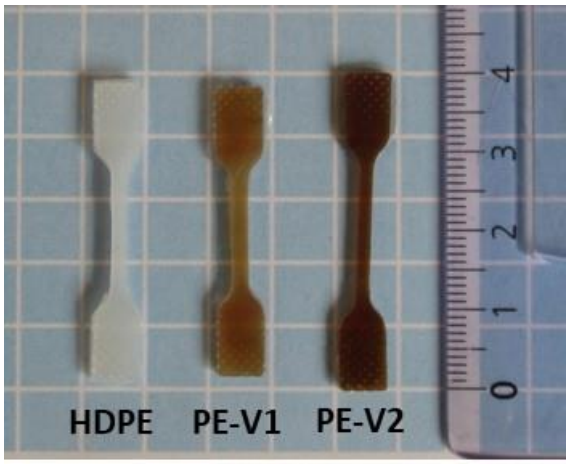

Fig. S10 Photographs of HDPE, PE-V1 and PE-V2. Scale in cm on the right.

4. Quantification of the degree of crystallinity by DSC

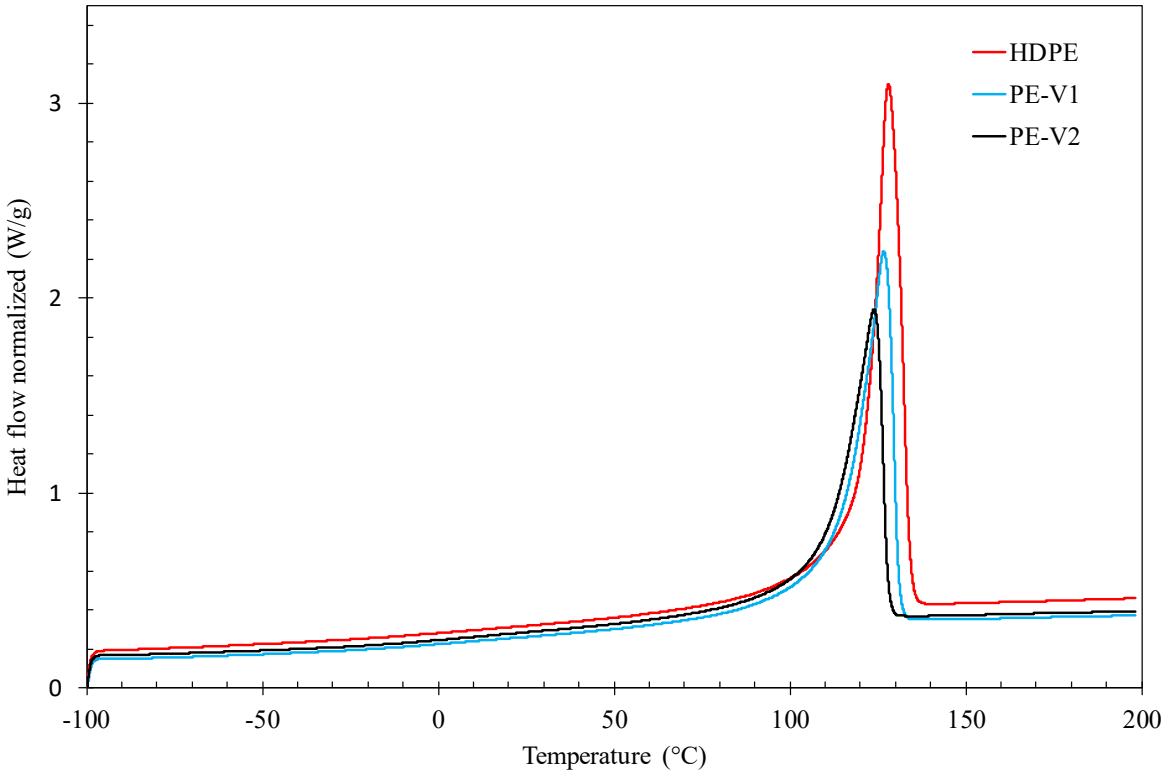

Fig. S11 DSC of HDPE, PE-V1 and PE-V2.

Table S1 Melting point and degree of crystallinity of HDPE, PE-V1 and PE-V2 determined by DSC.

	Melting point (°C)	Melting enthalpy (J/g)	Degree of crystallinity (%)
HDPE	128	185	64.2
PE-V1	127	151	52.4
PE-V2	124	127	44.1

The degree of crystallinity χc was calculated from the specific enthalpy of melting ΔHm as $\chi c = \Delta Hm / \Delta Hm^*$, where $\Delta Hm^* = 288$ J.g^{-1} corresponds to the specific enthalpy of melting of a fully crystalline polyethylene.

5. Stress relaxation on PE-V1 and zero shear viscosities of HDPE, PE-V1 and PE-V2

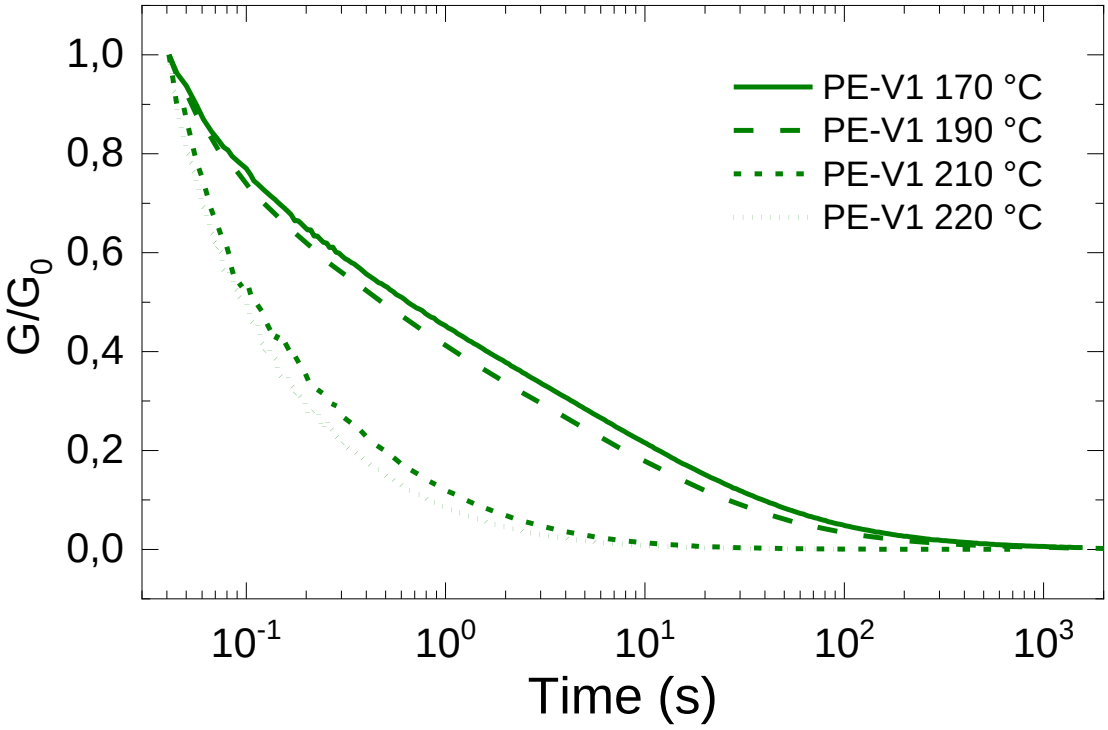

Fig. S12 Normalized stress relaxation profiles (1% strain) of PE-V1 at different temperatures.

Table S2 Zero shear viscosities of HDPE, PE-V1 and PE-V2 vitrimers calculated from stress relaxation experiments

	HDPE	PE-V1	PE-V2
T (°C)	η_0 (Pa.s)	η_0 (Pa.s)	η_0 (Pa.s)
160	-	3.69×10^6	2.23×10^7
170	1.20×10^4	4.27×10^6	1.66×10^7
180	-	3.96×10^6	1.33×10^7
190	8.42×10^3	3.35×10^6	8.77×10^6
200	-	5.35×10^5	3.41×10^6
210	6.14×10^3	4.19×10^4	1.01×10^6
220	-	1.74×10^4	2.54×10^4
230	4.73×10^3	8.79×10^3	-

6. FTIR characterization of PE-V1 and PE-V2 after annealing at 250 °C

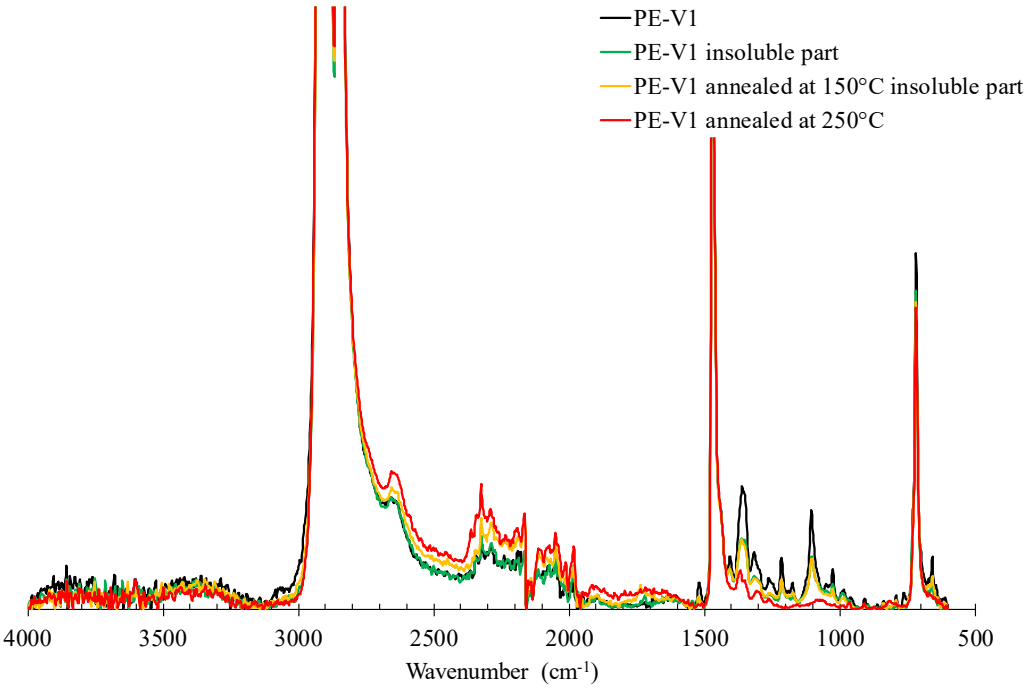

Fig. S13 FTIR spectra of PE-V1 as extruded (black), of the insoluble part PE-V1 (green), of the insoluble part of PE-V1 after thermal annealing at 150 °C (yellow) and of PE-V1 after a thermal annealing at 250 °C followed by precipitation (red).

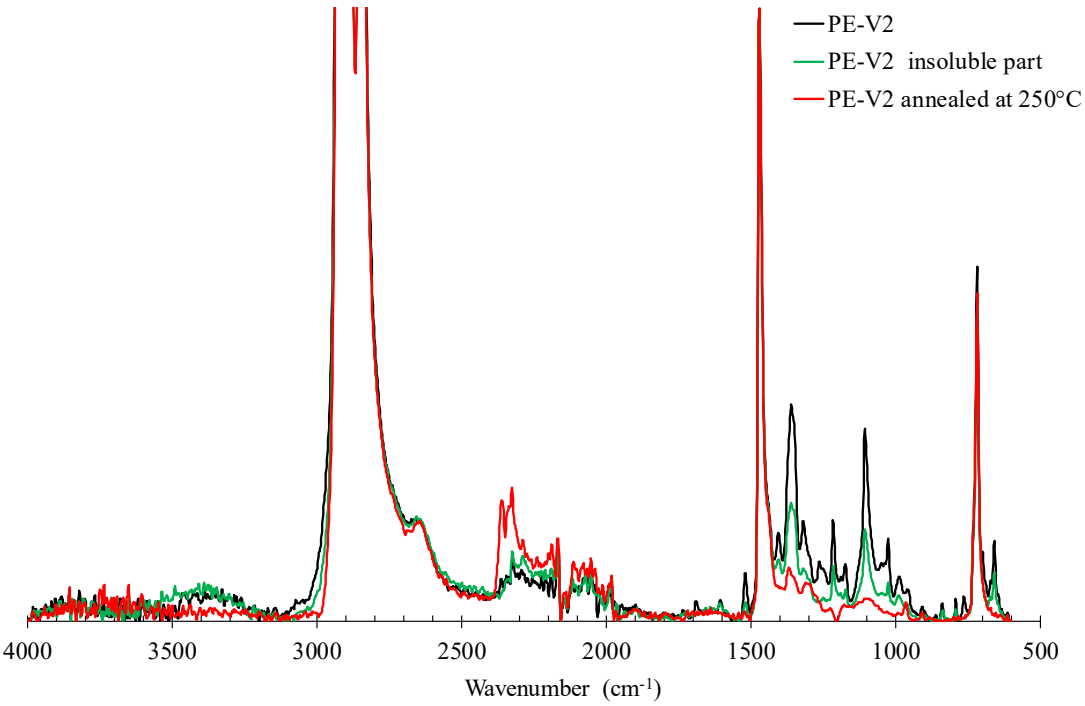

Fig. S14 FTIR spectra of PE-V2 as extruded (black), of the insoluble part PE-V2 (green) and of PE-V2 after a thermal annealing at 250 °C followed by precipitation (red).

7. Strain sweep experiments on PE-V1 and PE-V2

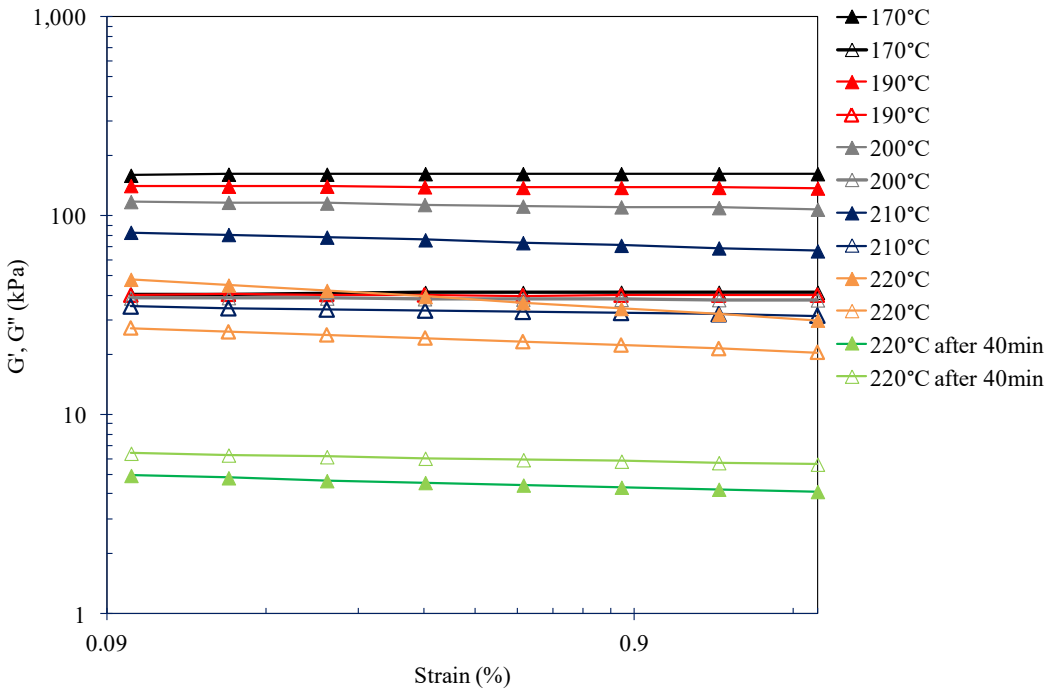

Fig. S15 Variation of storage and loss modulus of PE-V2 at different temperatures with strain amplitude under an angular frequency of 1 rad.s^{-1}.

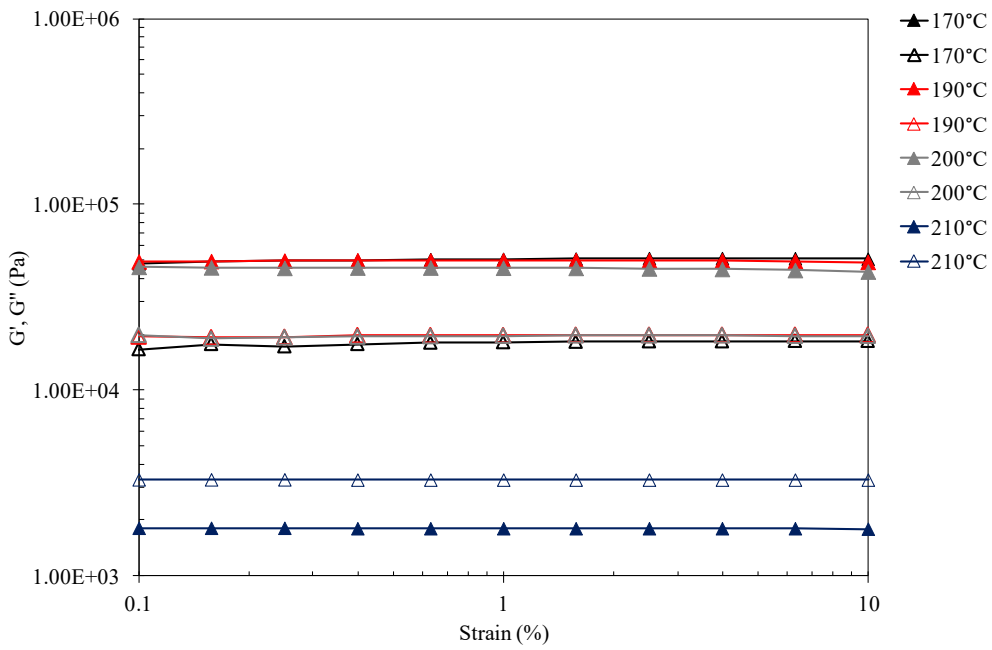

Fig. S16 Variation of storage and loss modulus of PE-V1 at different temperatures with strain amplitude under an angular frequency of 1rad.s^{-1}.

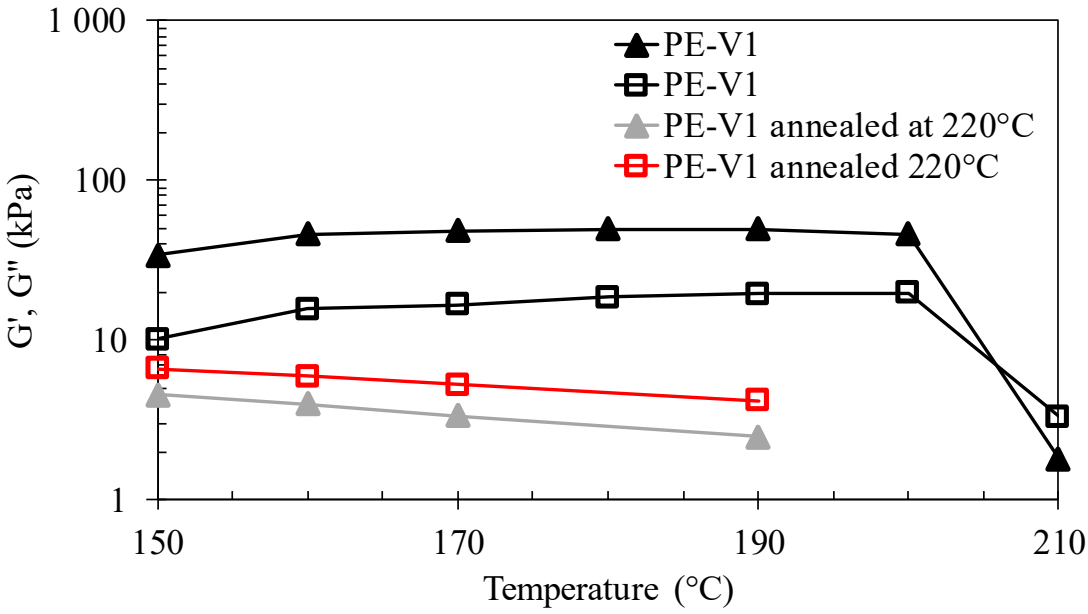

Fig. S17 Storage (triangle) and loss (square) modulus of PE-V1 before and after annealing at 220 °C as a function of temperature with an angular frequency of 1 rad.s^{-1} and a strain of 0.1%.

8. Mechanical properties of HDPE, PE-V1 and PE-V2

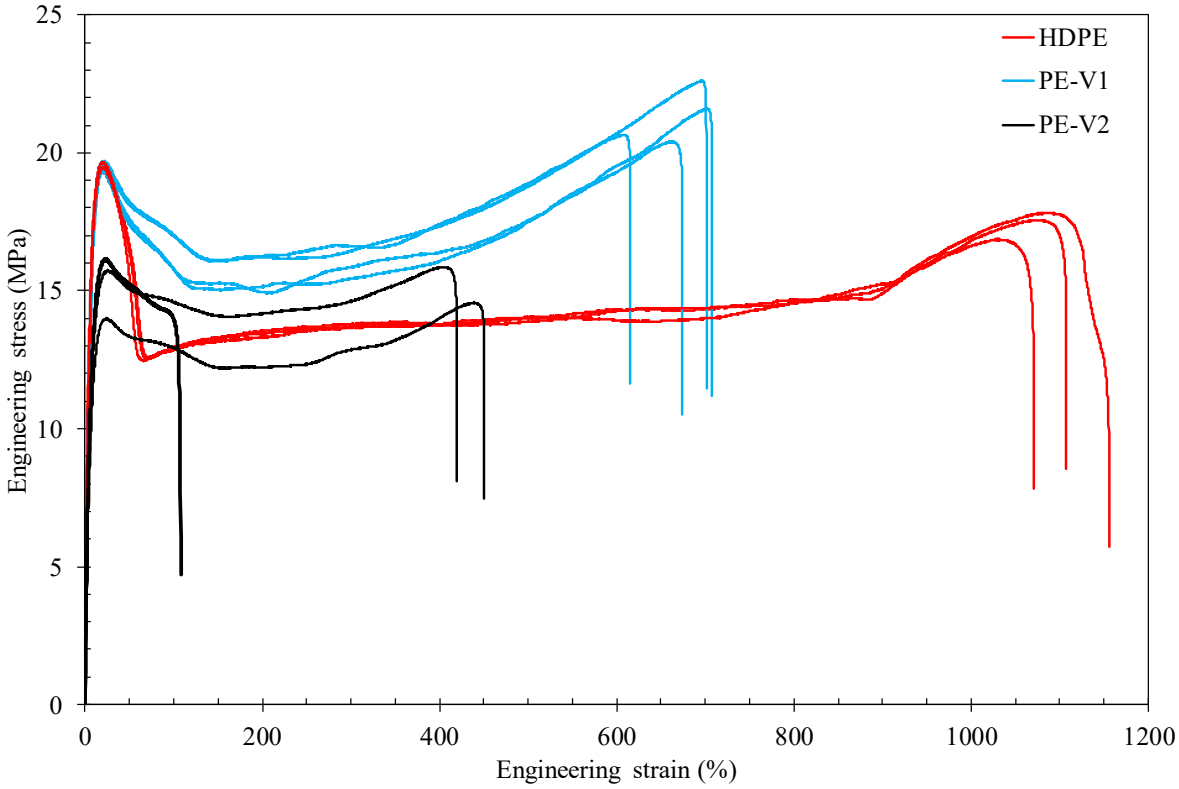

Fig. S18 Tensile stress-strain curves at RT for the HDPE precursor, PE-V1 and PE-V2.

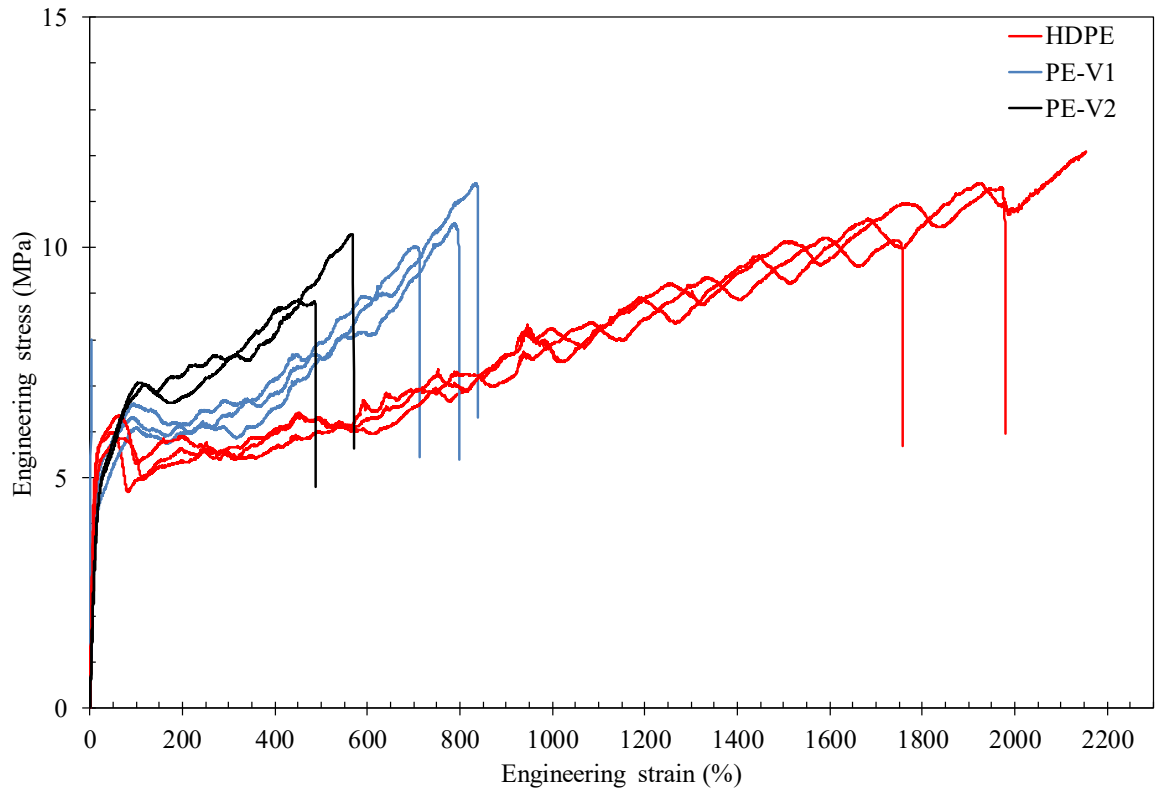

Fig. S19 Tensile stress-strain curves at 80 °C for the HDPE precursor, PE-V1 and PE-V2.

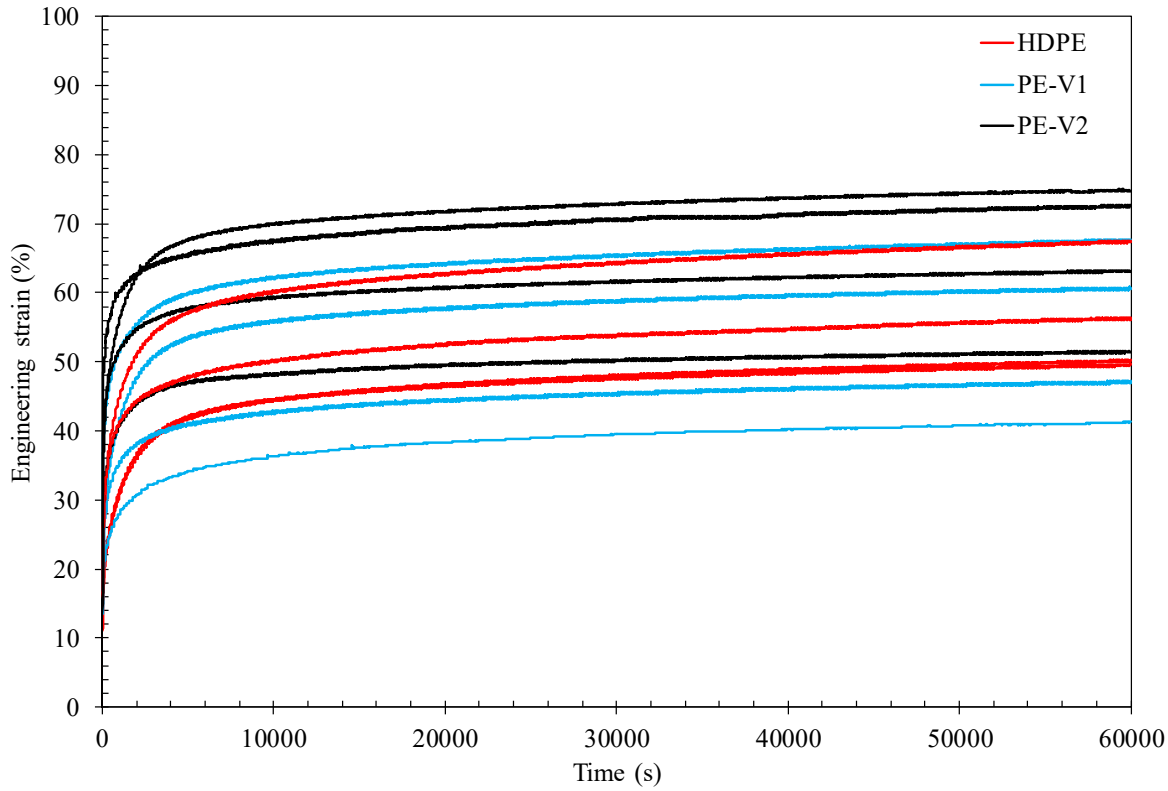

Fig. S20 Elongational creep tests at 80 °C and 5 MPa for the HDPE precursor (in red), PE-V1 (blue) and PE-V2 (grey) vitrimers. Results on 4 specimens are shown for reproducibility.